Effect of frequency of air flow on the performance of the Wells turbine

S. Raghunathan and O. O. Ombaka*

Experimental investigations on the effect of Strouhal number and rotor solidity on the performance of 0.2 m diameter Wells self rectifying air turbine with NACA 0021 profile blades are presented. The results show an increase in starting torque with the Strouhal number of air flow and rotor solidity. The effect of Strouhal number on the running performance of the turbine is solidity dependent

Keywords: *turbomachinery, fluid flow, wave energy*

The Wells air turbine is a self-rectifying air turbine suited for wave energy conversion from the oscillating water-air column devices. Some recent reports[1-3] explain the principle of the working of turbine, the starting characteristics, the prediction of the performance and the effect of several variables on the running performance of the Wells turbine. Some initial experiments on the Wells turbine in an oscillating air flow have been reported[4]. The starting and running performance of a 0.2 m Wells turbine at several air flow frequencies and two solidities are reported here. The results are correlated with the results from unidirectional (zero frequency) air flow tests.

Experiments

Experiments were performed in an oscillating flow rig (Fig 1) consisting of an air bellow driven by a ram and hydraulic jack. The frequency of the jack which produced air oscillations was controlled by a signal generator and servo-amplifier system, the vertical displacement of the piston being controlled by limit switches. The test section with a 0.2 m diameter Wells turbine was mounted on top of the test rig. The model configurations chosen for the tests were (i) $h=0.65$ and $S=0.69$ and (ii) $h=0.65$ and $S=0.52$. Both models had 0.09 m chord blades with NACA 0021 aerofoil sections. All the tests were carried out at $R=2.5\times10^5$ for running conditions and $R_x=5.5\times10^4$ for starting conditions.

The measurements consisted of velocity profiles on both sides of the rotor, pressure drops across the rotor, turbine torque and speed. Velocity profile traversing stations 1 and 2 are shown in Fig 1. A CTA anemometer (DISA type 55M10) with a lineariser (type 55D10) and a calibrated hot wire probe (P11) was used for the velocity measurements. The pressure drop was measured by a low differential pressure transducer (Furness Control type FC040) which had frequency response up to 50 Hz. The torque was measured by a torque transducer (ASL DORT1). An optical type tachometer was used for the speed measurements. The data acquisition system consisted of a digital PAC 11/16 utilising a DEC LSI 11/2 microprocessor with a VT 50 graphic terminal and a Data Dynamics printer.

Tests were performed at several oscillating flow frequencies and several pressure drops. Some measurements were also made with the turbine rotor in a locked position (zero speed).

Running performance

Typical rotor pressure drop-time, ($\Delta p \sim t$) and inlet axial velocity-time ($V_x \sim t$) histories obtained during the tests were shown in Fig 2. These were close to sine waves. The variation of turbine torque τ and speed ω, (Fig 3) with time over the mean values was within $\pm4\%$ and $\pm2\%$ respectively. The power output variation with time was $\pm6\%$. Fig 4 shows that at any given instant the inlet axial velocity was almost constant with the radius within the annulus. These figures are discussed in more detail elsewhere[4]. From the oscillating air flow tests the values of p^*_{RMS}, W^*_{av}, η_{av} and ϕ_{RMS} for a cyclic period T can be obtained as follows:

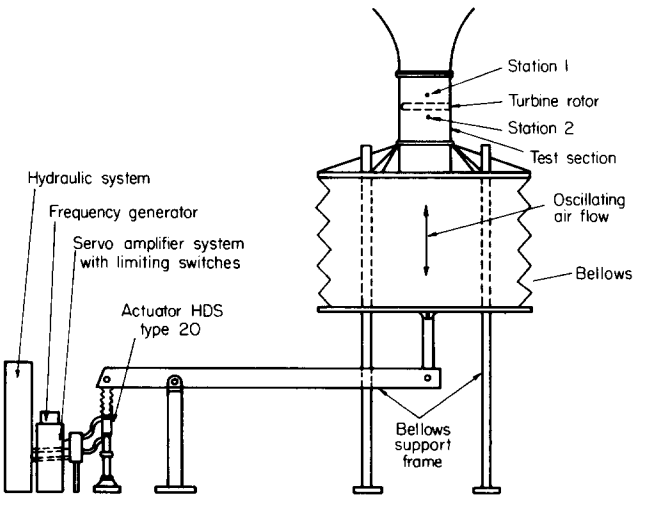

Fig 1 Oscillating air flow rig

* Department of Aeronautical Engineering, Queen's University of Belfast, Belfast, Northern Ireland
Received 4 June 1984 and accepted for publication on 6 September 1984

$$p^*_{RMS}=\frac{1}{\rho\omega_{av}^2 D_t^2}\left[\int_0^1 \Delta p^2\, d\left(\frac{t}{T}\right)\right]^{1/2} \quad (1)$$

is the root mean square pressure drop;

$$W^*_{av}=\frac{1}{\rho\omega_{av}^3 D_t^5}\int_0^1 \omega\tau\, d\left(\frac{t}{T}\right) \quad (2)$$

is the nondimensional average power output;

$$\eta_{av}=\frac{\int_0^1 \omega\tau\, d\left(\frac{t}{T}\right)}{\int_0^1 \Delta pQ\, d\left(\frac{t}{T}\right)} \quad (3)$$

is the average cyclic efficiency, and:

$$\phi_{RMS}=\frac{2}{\omega_{av}D_t}\sqrt{\int_0^1 V_x^2\, d\left(\frac{t}{T}\right)} \quad (4)$$

is the root mean square flow coefficient where:

$$\omega_{av}=\int_0^1 \omega\, d\left(\frac{t}{T}\right)$$

is the average speed, τ is the torque, and $R=U_t c/\nu$ is the Reynolds number based on the tip speed which, as the variation in speed was within $\pm 2\%$, was assumed constant.

Fig 5 shows plots of p^* versus ϕ_{RMS} for a range of oscillating flow frequencies from 0.2 to 1 Hz and for two solidities, 0.52 and 0.69. Also shown are the results from unidirectional flow tests (zero frequency). It can be observed that generally a linear relationship exists between p^* and ϕ_{RMS}. The effect of increasing airflow frequency on p^* is not very evident from this graph

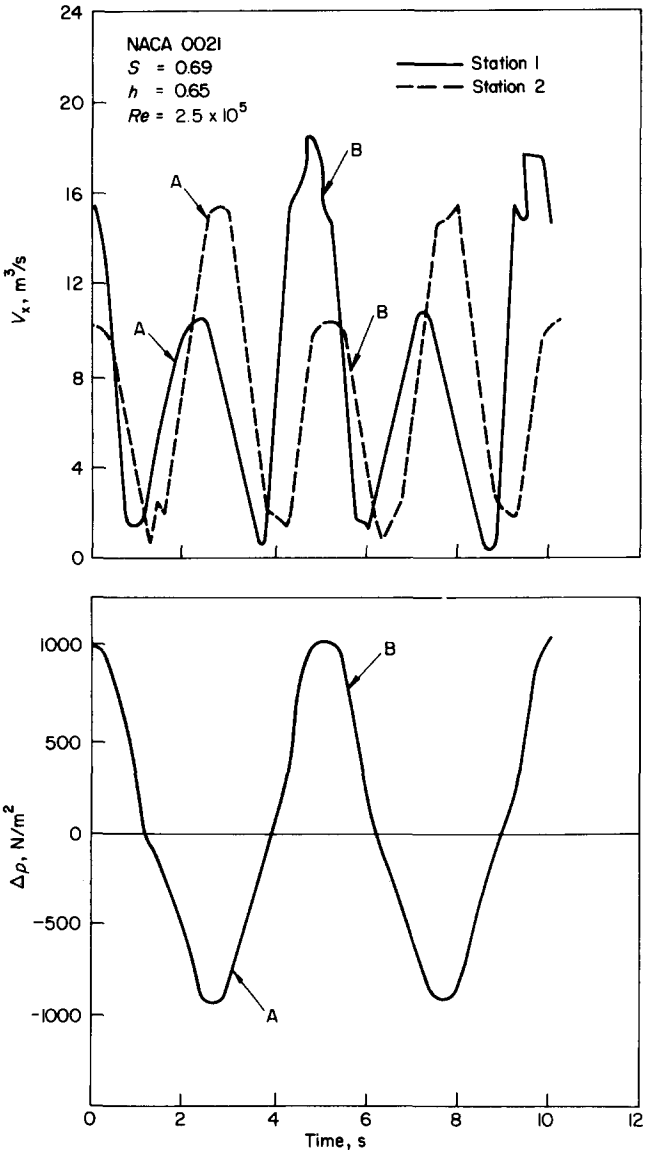

Fig 2 Pressure drop and axial velocity histories

Notation

c	Blade chord length, m
$C_{L,D}$	Lift, drag coefficient
$D_{t,h}$	Tip, hub diameter of the rotor, m
f	Frequency of oscillations, Hz
h	Hub to tip ratio D_h/D_t
n	Number of blades
$p^*, \overline{\Delta p}$	Pressure drop coefficient $\frac{\Delta p}{\rho\omega_{av}^2 D_t^2}, \frac{\Delta p}{\frac{1}{2}\rho V_x^2}$
Δp	Pressure drop across rotor, N/m²
Re, Re_x	Reynolds number $U_t c/\nu$, $V_x c/\nu$
S	Solidity $2nc/(\pi D_t(1+h))$
S_t, S_x	Strouhal number fc/U_t, fc/V_x
t	Time, s
T	Period for a cycle,
V_x	Axial velocity, m/s
W^*	Power coefficient, $W_0/\rho\omega_{av}^3 D_t^5$
U_t	Tip tangential velocity at rotor, m/s
α	Angle of incidence $=\tan^{-1}(V_x/U_t)$, degrees
ρ	Density of air, kg/m³
ω	Angular velocity, rad/s
ν	Kinematic viscosity of air, m²/s
η	Gross efficiency W_0/W_I
$\tau, \bar{\tau}$	Torque Nm, reduced torque, $\tau/\frac{1}{2}\rho V_x^2 nc(D_t^2/4)(1-h^2)$
τ^*	Torque coefficient, $\bar{\tau}/\Delta\bar{p}$
ϕ	Flow coefficient (V_x/U_t)

Subscripts

av	Average value
opt	Optimum value
rms	Root mean square value

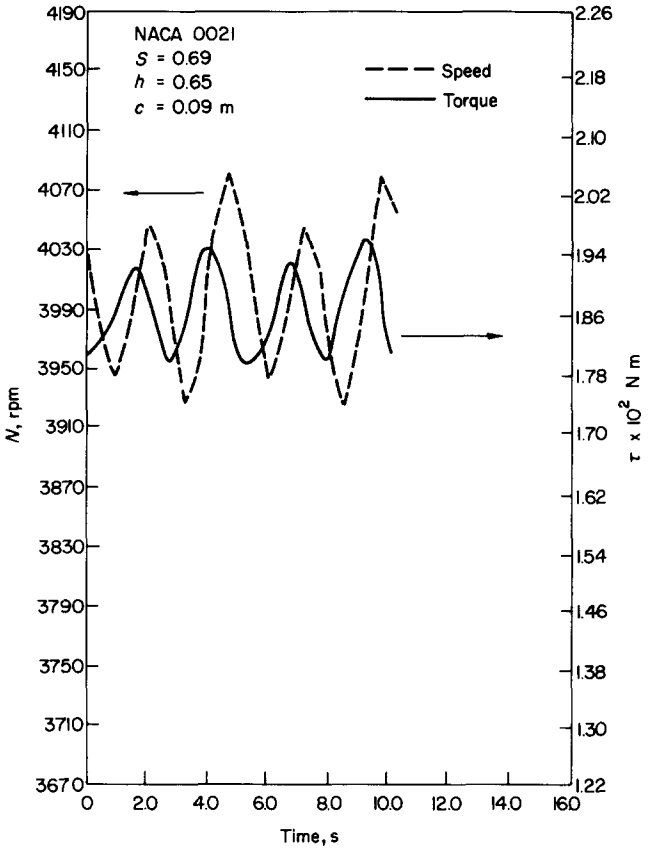

Fig 3 Torque and speed histories

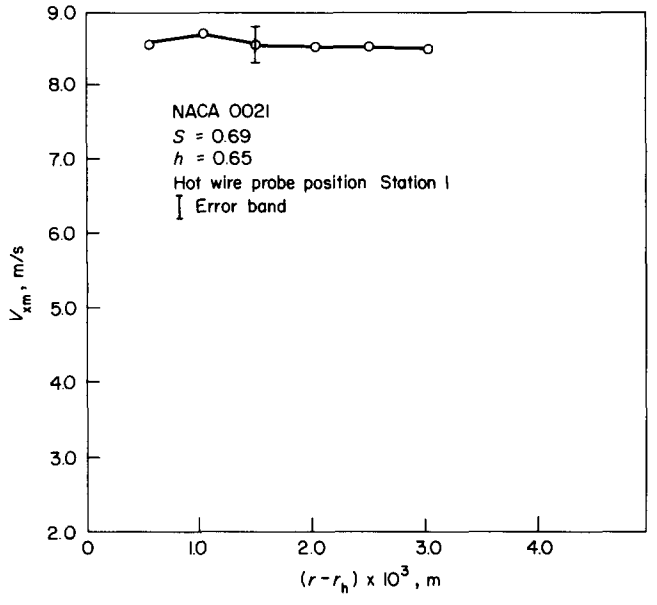

Fig 4 Annulus peak velocity distribution

although for a solidity of 0.52 the oscillating flow test results show a reduction in p^* compared with the unidirectional flow test results. Increase solidity produces an increase in pressure drop.

Fig 6 shows a deviation of oscillating flow test results from the unidirectional flow test results when the power outputs are compared. Once again, within the scatter of the data the effect of increase in f on W^* is not clear but it is apparent that the effect of flow oscillations is to increase W^* at the lower solidity of 0.52 and decrease

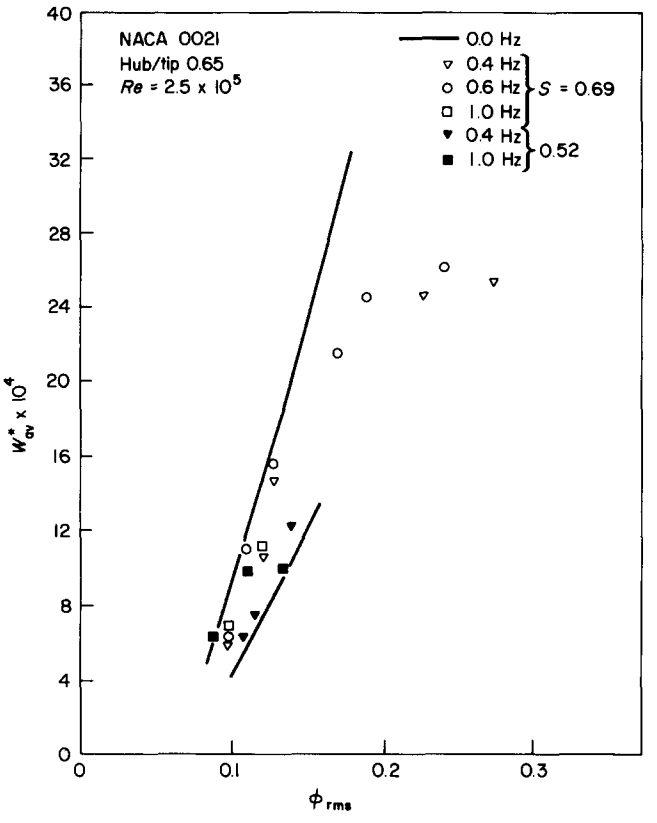

Fig 5 Effect of solidity on pressure drop

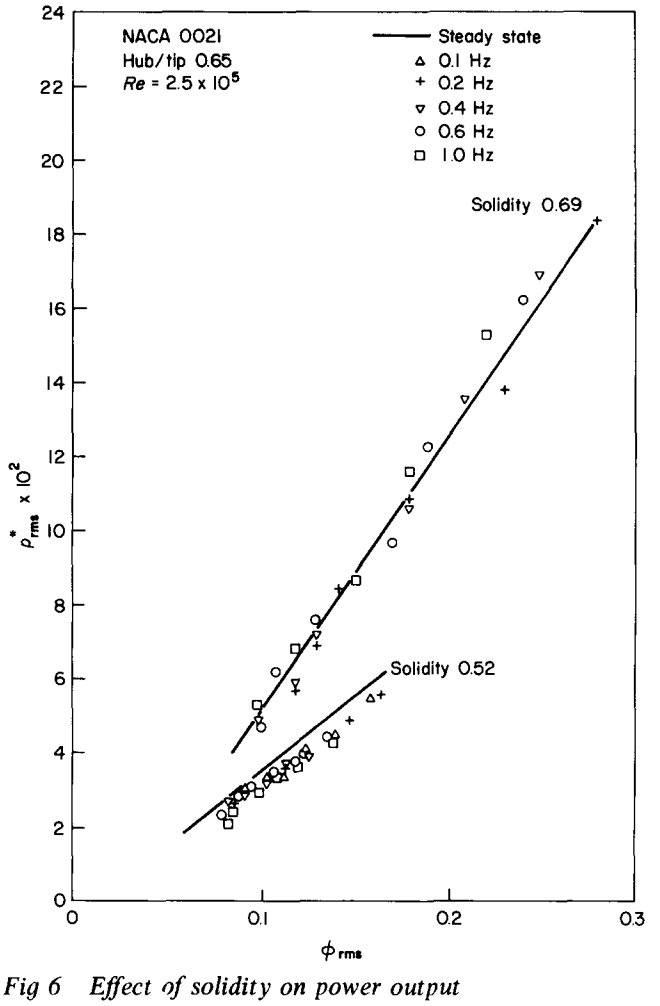

Fig 6 Effect of solidity on power output

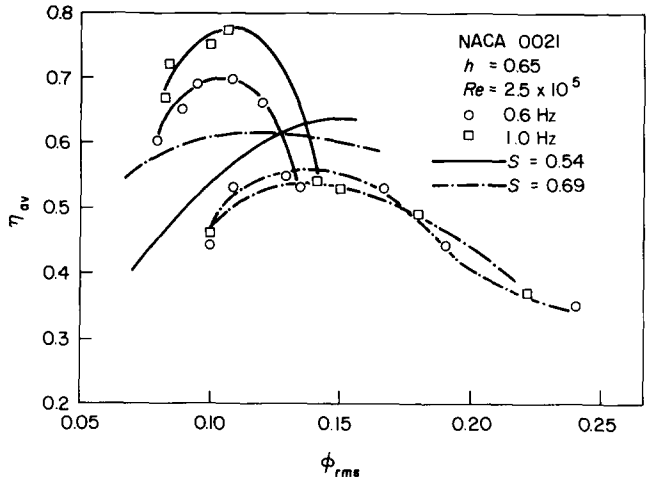

Fig 7 Effect of solidity on efficiency

W^* at a higher solidity of 0.69 when the results are compared with those at zero frequency. Stalling is very noticeable in this plot, with the increase in frequency promoting an earlier stall.

Increase in air flow frequency results in an improvement in efficiency at $S=0.52$ and reduction in efficiency at $S=0.69$ (Fig 7). The overall turbine solidity of 0.52 corresponds to a tip solidity of 0.43 where as $S=0.69$ corresponds to a tip solidity of 0.57. As a major part of energy conversion takes place nearer the tip rather than the hub, the tip solidity is a good representation of the turbine geometry. In this context, a tip solidity of 0.43 can be regarded as a low value and 0.57 as a high value. The results suggest that at low solidity the aerodynamic performance, which can be measured in terms of C_L/C_D, of the blades improves with the frequency of air flow oscillations. Although there are no wind tunnel tests available for a direct comparison, oscillating isolated aerofoil tests do show that the air flow oscillations produce hysteresis effects[5] which tend to postpone separation and therefore increase C_L/C_D and hence increase the aerodynamic performance of an aerofoil blade.

Bringing the blades to a close proximity, however, seems to produce a deterioration in the aerodynamic performance of the blades in an oscillating air flow as the results of the high solidity tests tend to show. This is possibly due to the fact that the wake shed by a blade lowers the C_L and increases C_D on a blade just behind it[6], ie on blades closely arranged in tandem cascade.

For a given frequency the efficiency of the turbine therefore reduces with the increase in solidity showing the reduction in aerodynamic performance of the turbine when the blades are brought closer to each other; efficiency increases when the blades are further apart.

The optimum pressure drop p^*_{opt} and the optimum power coefficient W^*_{opt} for maximum efficiency as a function of Strouhal number of air flow S_t for both the solidities are shown in Fig 8. In this non dimensional plot it is interesting to note that for both solidities the pressure drop decreases with the Strouhal number. However, at the high solidity the effect of Strouhal number on p^*_{opt} appears to be small. The $W^*_{opt}-S_t$ curves show a continuous drop in W^*_{opt} with S_t for both the solidities. The results from the oscillating flow tests correlate very well with the results from the unidirectional flow tests.

Fig 9 shows the effect of Strouhal number on the maximum value of cyclic efficiency, η_{max}, and the corresponding flow coefficient ϕ_{opt}. Improvement in η_{max} obtained at higher S_t for the low solidity has already been explained. Typically at $S=0.52$ and $S_t=10^{-3}$ an increase in η_{max} of 5–6% is observed when compared to the value of η_{max} at $S_t=0$. There is a corresponding reduction in η_{max} of 5–6% at $S=0.69$. These results show that there is an advantage in using a turbine of low solidity in oscillating air flows. Such a turbine, however, can only operate at low pressure drops, as seen earlier, and may not be self starting[2]. These curves also indicate that for $S=0.69$ the values of η_{max} may be independent of S_t for the operating region of the Wells turbine, that is $0<S_t<10^{-3}$. The optimum flow coefficient values ϕ_{opt} in Fig 9 show a larger sensitivity to S_t at the low values of S. This figure shows that the design value of ϕ must be somewhat lower than that based on unidirectional flow tests.

Starting torque

In order to understand the starting torque produced by an oscillating air flow, the turbine rotor was locked and the variation of torque τ at zero speed ω with pressure drop Δp and flow rate Q were measured at several air flow frequencies. Figs 10 and 11 show the variation of pressure drop with flow rate and torque with flow rate for two turbine solidities and frequencies of 0.2 Hz and 1 Hz and a constant average $R_x=5.5\times10^4$.

The results could be expressed in non-dimensional

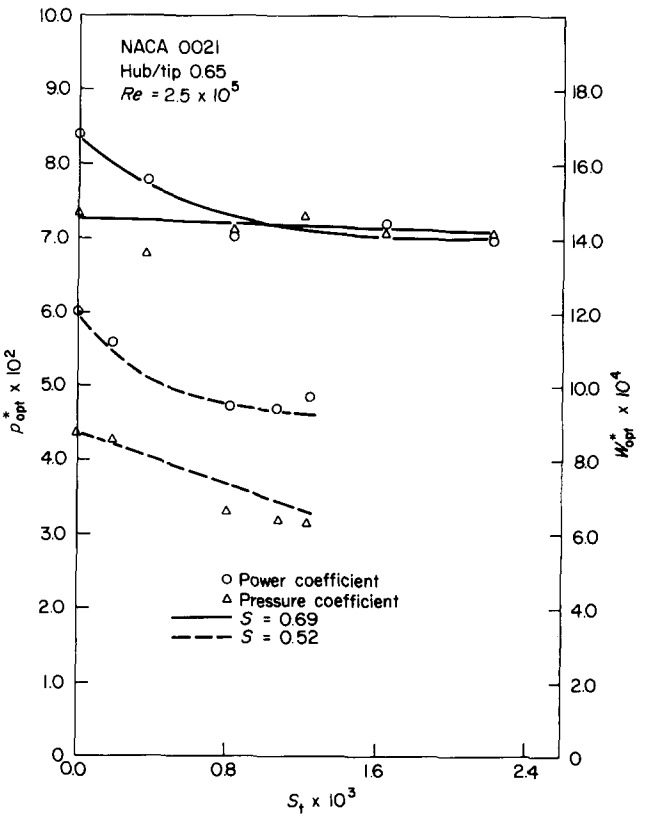

Fig 8 Effect of Strouhal number on optimum pressure drop and power output

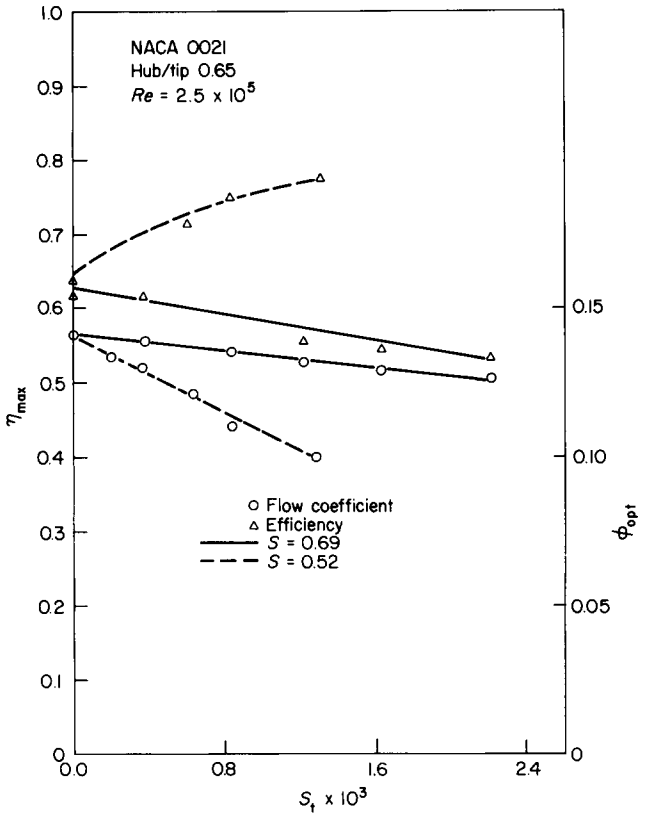

Fig 9 Effect of Strouhal number on efficiency and flow coefficient

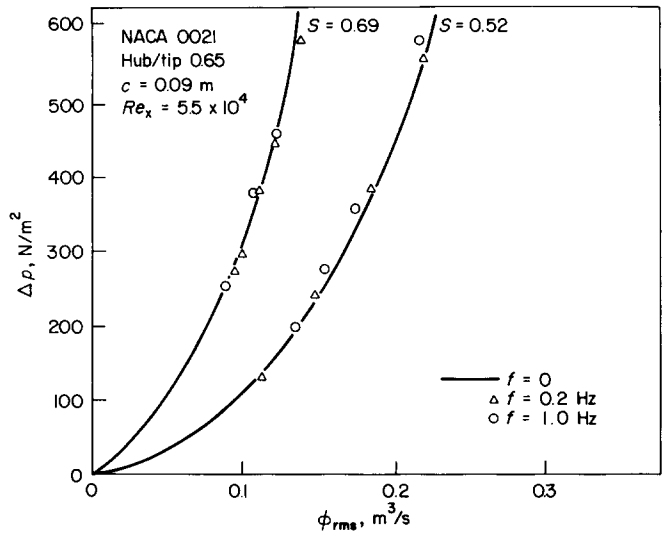

Fig 10 Variation of pressure drop with flow rate

form, viz pressure drop coefficient $\overline{\Delta p}$:

$$\overline{\Delta p} = \frac{\Delta p}{\frac{1}{2}\rho V_x^2} \tag{5}$$

reduced torque, $\bar{\tau}$:

$$\bar{\tau} = \frac{\tau}{\frac{1}{2}\rho V_x^2 n c D_{t/4}(1-h^2)} \tag{6}$$

torque coefficient, τ^*:

$$\tau^* = \frac{\bar{\tau}}{\overline{\Delta p}} \tag{7}$$

Strouhal number, S_x:

$$S_x = \frac{f_c}{V_x} \tag{8}$$

Reynolds number R_x:

$$R_x = \frac{U_c}{V_x} \tag{9}$$

It should be noted that the turbine blades are subjected to incidences ranging from $+90°$ to $-90°$ during these tests. Unpublished results from similar tests in a unidirection air flow rig are also shown. The $\Delta p \sim Q$ curves show a quadratic relationship ($\Delta p = KQ^2$) for all frequencies including $f=0$. The rotor behaves like an orifice plate when it is stationary and the constant of proportionality K is a function of solidity and is virtually independent of frequency at these low frequencies.

Fig 11 shows that there is a negligible effect of low frequencies on torque produced at a given flow rate for $S=0.52$ and $S=0.69$. It has been suggested that the trends could change at low solidities and high frequencies.

The true effect of air flow frequency on the turbine blades can be observed from Fig 12 where a non-dimensional value of torque $\bar{\tau}$ is plotted against a non-dimensional value of pressure drop $\overline{\Delta p}$ for several values

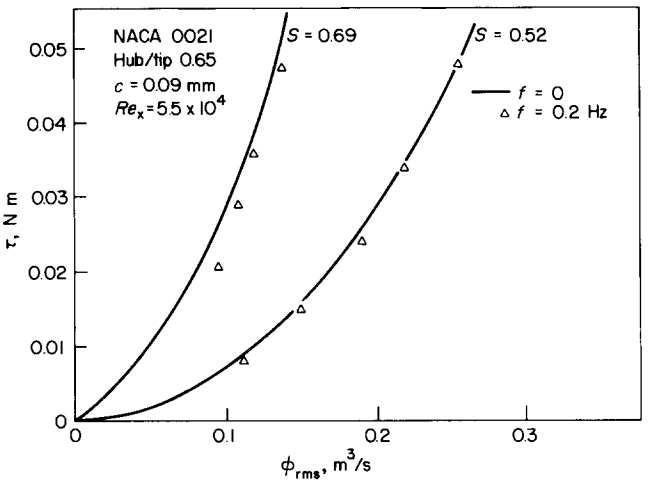

Fig 11 Variation of torque with flow rate

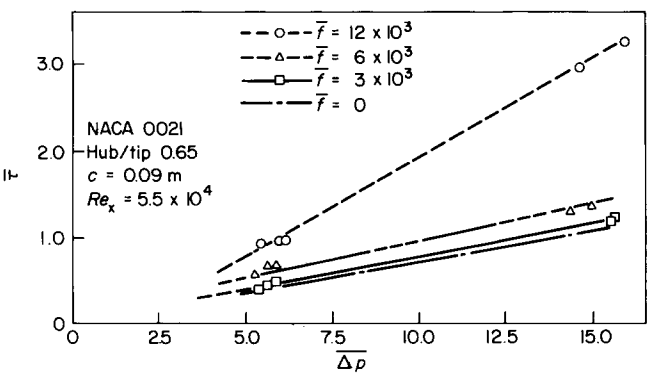

Fig 12 Variation of torque with pressure drop

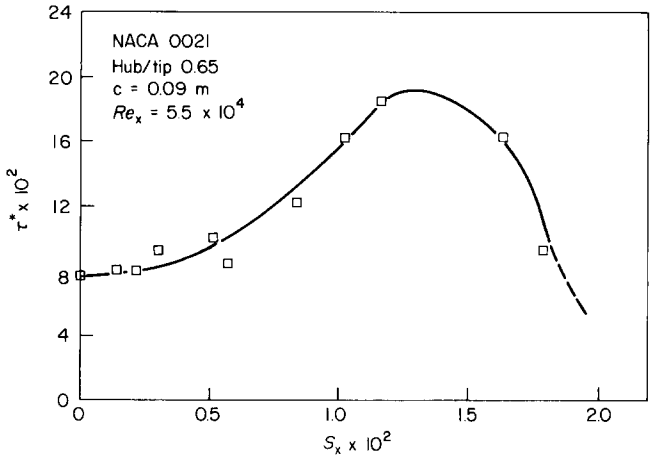

Fig 13 Variation of torque with Strouhal number

of Strouhal numer S_x based on axial flow velocity V_x. For a given value of S_x, $\bar{\tau}$ varies linearly with $\overline{\Delta p}$ and this is independent of S. For a given $\overline{\Delta p}$, $\bar{\tau}$ increases significantly with S_x. The values of $\bar{\tau}$ at $S_x = 12 \times 10^{-3}$ are twice those at $S_x = 0$. At starting, $\alpha = 90°$ and hence the value of tangential force coefficient C_t and axial force coefficient C_x are fixed for a given S, R_x and profile. $\bar{\tau}$ is equal to C_t and $\overline{\Delta p}$ is a function of both h and S. Since the value of h is constant, the increase in $\bar{\tau}$ with $\overline{\Delta p}$ is associated with the increase in S.

A unique relationship between the torque and frequency can be obtained if a coefficient of torque τ^* is plotted against S_x as shown in Fig 13. This correlation is independent of solidity, pressure drop and flow rate and is a function of S_x only. A rapid increase in τ^* with S_x is noticeable from this figure but only up to a value of $S_x = 1.25 \times 10^{-2}$ beyond which there is a sharp reduction in τ^*. As most of the wave energy devices are likely to operate with $S_x < 10^{-2}$, the drop in τ^* with S_x at high frequencies is not important. Therefore this curve suggests that considerably higher starting torque is achieved in oscillating air flow than that predicted from unidirectional flow tests.

Conclusions

The performance of the Wells self-rectifying air turbine in oscillating air flow is presented in this paper. The running performance in oscillating air flow is solidity dependent. Increase in solidity produces an increase in pressure drop and reduction in maximum efficiency. Increasing the frequency of air oscillation results in an increase in power output and efficiency for low solidity and vice versa for high solidity. The oscillating air flow produces a higher starting torque than a unidirectional air flow.

Acknowledgement

The authors wish to thank the Department of Energy, United Kingdom, for financial support for these investigations.

References

1. **Raghunathan S. and Tan C. P.** Aerodynamic performance of a Wells air turbine, *J. Energy, 1983*, **7**(*3*), *226–230*
2. **Raghunathan S. and Tan C. P.** Performance of Wells turbine at starting, *J. Energy, 1982*, **6**(*6*), *430–431*
3. **Raghunathan S. and Tan C. P.** Performance prediction of the Wells self-rectifying air turbine, *to be published in 19th Intersociety Energy Conversion Engineering Conference, in San Francisco, Aug 1984*
4. **Raghunathan S. and Ombaka O. O.** The Wells turbine in an oscillating air flow, *to be published in 19th Intersociety Energy Conversion Engineering Conference, San Francisco, Aug 1984*
5. **McAlister K. W., Carr L. W. and McCroskey W. J.** Dynamic stall experiments on NACA 0012 airfoil, *NASA TP 1100, Jan 1978*
6. **Scholz N.** Aerodynamics of cascades. *AGARDOGRAPH – 220, Trans. by A. Klein, 1977, 280*